SciMedCentral

Annals of Vascular Medicine & Research

Research Article

Cardiac MRI Characterization of the Left Ventricle after Pulmonary Vein Isolation

Britta Elkenhans[1]*, Ingmar Vieregge[2], Markus Henningsson[3], Tarique Muhammad Hussain[4], Rene Botnar[5], and Gerald Greil[4]

1Department of Cardiology, University Hospital Duesseldorf, Germany
2Department of Cardiology, University of Luebeck, Germany
3Department of Cardiology, Linköping University, Sweden
4Department of Cardiology, UT South western, Dallas, USA
5Department of Imaging Sciences, King's College London, UK

***Corresponding author**
Britta Elkenhans. MD, Department of Cardiology, University Hospital Duesseldorf, Moorenstr 5, 40225 Duesseldorf, Germany, Tel: +49-(0)179-31445067

Submitted: 03 November 2023
Accepted: 30 November 2023
Published: 30 November 2023
ISSN: 2378-9344

Abstract

Background: Atrial fibrillation is a disease that is common in developed countries, which can cause impaired systolic function due to regional and global wall motion abnormalities. The symptoms hinder everyday life by dyspnoea and palpitations, which are classified by ERHA (European heart rhythm association score of atrial fibrillation). nMARQ™ was recently introduced as a means of pulmonary vein isolation (PVI); this single-shot device facilitates a quick and safe procedure that generates scar tissue in the left atrium to prevent the conduction of inappropriate electrical signals. Our aim was to characterize the left ventricle with the assessment of global and regional wall motion abnormalities before and after PVI by SENC (strain encoded cardiac imaging) in cardiac MRI.

Methods: Twenty atrial fibrillation patients referred for PVI were prospectively enrolled in the study between December 20212 and March 2015 at the University of Duesseldorf with symptomatic atrial fibrillation ERHA III (severe symptoms, normal daily activity affected). Cardiac magnetic resonance imaging (cMRI) was performed using a 1.5-Tesla MR scanner one day before, one day after and three months after the patients underwent PVI with nMARQ. We conducted a standard balanced steady-state free precession (SSFP) sequence to assess left and right ventricular volumes. Strain-encoded (SENC) imaging was performed in four- and two-chamber views to assess the longitudinal strain on the left ventricle. Late gadolinium enhancement (LGE) imaging was performed 10 min after administration of a contrast agent. The one-month follow-up characterization of the left ventricle was conducted with the identical cMRI protocol described above.

Results: No adverse events occurred. The average ejection fraction before PVI was 57%; the left ventricle had a diastolic volume of 135 mL and a systolic volume of 58 mL, and the myocardial mass was 155 g. Three months after PVI, the global and regional strain on the left ventricle were significantly reduced relative to pre-PVI levels ($p<0.002$ and $p<0.03$, respectively).

Conclusion: In this study, the nMARQ system achieved safe PVI that improved quality of life (EHRA I)(no symptoms) in patients with atrial fibrillation. When atrial fibrillation was eliminated, we observed functional recovery of the left ventricle as measured by global and circumferential strain and restoration of the sinus rhythm one month after PVI.

INTRODUCTION

Atrial fibrillation is a common disease in developed countries that compromises patients' daily lives due to dyspnoea and palpitations. The common causes of the symptoms are regional and global wall motion abnormalities of the left ventricle which can lead to impaired left ventricular function [1]. First-line therapy includes anti-arrhythmic drugs, such as beta blockers, often used in combination with anticoagulants. If pharmaceutical treatment fails to restore quality of life, pulmonary vein isolation (PVI) is a surgical option to restore normal activity.

PVI was first introduced by Michael Haissaguerre in 1998, who identified the pulmonary veins as important to the initiation of atrial fibrillation [2]. The goal of PVI is to generate a scar in the left atrium that reduces the conduction of abnormal electrical impulses [3]. Several PVI techniques have been developed, resulting in iterative improvements in safety and procedure times. Earlier methods included cryoballoons [4] and robotic systems [5]; more recently, in 2011, the nMARQ™ system was introduced [6]. Its circular, multielectrode catheter is a single-shot system (Bioscience Webster, Inc., Diamond Bar, CA, USA) that creates durable and consistent lesions around the pulmonary veins [2].

The stabilization of regional wall motion abnormalities following PVI likely promotes functional recovery, but the process is not well understood. Previous studies indicated that speckle tracking with cardiovascular ultrasound is a reliable tool for the investigation of regional wall motion abnormalities [7]. Feature tracking is commonly used for the analysis of global strain analysis in cardiac MRI [8]. However, advances in cardiac magnetic resonance imaging (cMRI) of deformed myocardial tissue are now frequently used corporately with transthoracic echocardiography to support and refine the assessment of heart

failure; in particular, strain-encoded (SENC) imaging, which was first introduced in 2003 [9], may provide additional information on the underlying mechanism for this functional recovery regarding global and circumferential strain.

In this study, we aimed to examine the functional recovery of the left ventricle from atrial fibrillation after PVI with the nMARQ system. To better characterize the resolution of wall motion abnormalities after PVI in atrial fibrillation patients, we compared global *and* circumferential left ventricular wall motion with SENC one day prior to and one day and one month after PVI with nMARQ.

METHODS

Study population

This study prospectively recruited 20 patients (age 60 -+2) with atrial fibrillation under beta-blocker-therapy. The patients were interviewed regarding their symptoms (quality of life, EHRA-classification). Only patients with EHRA III underwent PVI. The study was conducted at the University Hospital in Duesseldorf, Germany, between December 2012 and March 2015. Exclusion criteria included any contraindication to cMRI, including implanted permanent pacemakers and implanted cardioverter-defibrillators. Institutional Review Board approval was obtained prior to the commencement of recruitment.

PVI protocol

The patient was informed to fasten and withholding of liquid intake for 12 hours. Afterwards, the patient was positioned in prone position and general anaesthesia with Midazolam (ratiopharm, Ulm, Germany) (0.15-0.2 mg/kg) and Fentanyl (Hexal, Holzkirchen, Munich, Germany) (2ug/kgKG) was administered intravenous. For PVI, a long catheter was first inserted into the common iliac vein (SJM SLI 8.5F). Subsequently, a positing system was inserted with an 8-pole electrode catheter (Inquiry 6F) for placement into the coronary sinus. At this point, distal atrial ablation sequences were examined for proof of the postpacing interval at the coronary sinus and at the cavotricuspid isthmus. A transseptal puncture (SJM BRK 71 cm) was then conducted, followed by angiography of the left atrium, which can indicate an increase in chamber size due to atrial fibrillation. Additionally, the septal pulmonary veins were reconnected, and the lateral pulmonary veins were isolated. Pulmonary vein presentation was visualized with the aid of contrast agent (Visipaque, Guerbet GmbH, Sulzbach/Taunus, Germany). Then, a diagnostic catheter (Lasso or Pentaray, Biosense Webster) was inserted along with an ablation catheter (Biosense Webster Navister Smart Touch F) into the left atrium. A three-dimensional reconstruction of the left atrium was established with the aid of CARTO3 (Biosense Webster). Here, roof-dependent atrial tachycardia was usually detected, and a circumferential ablation line was inserted into the septal and lateral pulmonary veins; evidence of block was observed afterwards at the line. After the procedure, the catheters were explanted. Two consultant cardiologists with at least more than ten years of experience conducted the procedure.

cMRI protocol

One day prior to, one day and one month after PVI, patients were scanned on a 1.5-Tesla Philips Achieva scanner with a 32-channel coil. Multislice, multiphase cine imaging was performed using a standard steady-state free precession (SSFP) pulse sequence in the short axis (voxel size 1.48 × 1.48 × 8.0 mm^3 to cover the entire left and right ventricle, TR 3.2, TE 1.59, flip angle 60°). Late gadolinium enhancement (LGE) imaging (voxel size 1.37 × 8.0 × 8.0 mm^3, TR 3.8, TE 1.86, flip angle 15°) was performed following a Look-Locker sequence (inversion time scout) 10 min after administration of contrast agent (0.2 mmol/l Dotarem, Guerbet, Villepinte, France). Left and right ventricular volumes, myocardial mass, and myocardial scarring were analysed at the Philips workstation (EWS, release 3.2.2, Philips, Best, the Netherlands) with the aid of LGE in short-axis, four-chamber, two-chamber and three-chamber views. SENC was conducted [10] in four- and two-chamber views to investigate longitudinal strain. SENC MRI of the left ventricular long axis two- and four chamber view were conducted to calculate longitudinal strain and SENC images of the short axis were performed to measure circumferential strain.

One day after PVI, a digital subtraction angiography was conducted to exclude damages after the procedure.

cMRI analysis

Endocardial and epicardial borders were manually contoured at end diastole and end systole to allow the calculation of ventricular volume and mass [epicardial volume – endocardial volume × myocardial density (1.05 g/cm^3)]. Values were indexed to body surface area. LGE areas were measured and indexed for normal myocardium and interpreted by calculating the segmental extent of LGE on short-axis planes at baseline. Areas of LGE were determined with respect to the transmural extent of the defect.

To measure longitudinal and circumferential strain, the left ventricle was divided into 12 segments [10] and analysed with dedicated software (Diagnosoft MAIN version 1.06, Diagnosoft Inc. Palo Alto, Calif.). For strain analysis, SENC was used to calculate changes in the frequency of a tag pattern within each voxel and provide measurements of circumferential and longitudinal strain.

The interobserver variability of the measurements of circumferential and longitudinal strain were assessed by two independent observers, who exhibited at least five years of MRI experience in a blinded and random order.

Follow-up

One month after PVI, the patients were interviewed regarding their symptoms (quality of life, EHRA-classification) and they underwent cMRI with SENC.

Statistical analysis

The chi-square test and Fisher's exact test were used to compare normally distributed variables. Student's t-test and

the Mann-Whitney U test were used to compare nonparametric variables. P-values less than 0.05 were considered statistically significant. Data were analysed using Graph Pad Prism (version 5, La Jolla, CA 92037, USA).

RESULTS

20 patients were investigated. Exclusion criteria were any contraindications for cMRI, like pacemakers. The patient characteristics are summarized in Table 1 and included comorbidities, such as cardiovascular disease, hypertension, diabetes and COPD.

Hemodynamic parameters

Before PVI, cMRI results revealed that the average ejection fraction was 57%, the left ventricular diastolic volume was 135 mL, the left ventricular systolic volume was 58 mL, and the myocardial mass of the left ventricle was 155 g Table 2.

Pulmonary vein isolation

We sought to perform PVI via the nMARQ system to alleviate the symptoms of atrial fibrillation in our patients. Figure 1a-d shows exemplary images of left atrium segmentation using the nMARQ system. Figure 2 a exhibits a reconstruction of the aorta and pulmonary veins to exclude damages after the PVI procedure.

Figure 2b-d shows a representative patient image taken in a "five-chamber" view (a 4-chamber view with the aortic valve).

Table 1: Patient characteristics

Study population	N=20
CVD	4
Previous myocardial infarction	0
Previous CABG	1
Previous PCI	3
Age (median)	60 (±2)
Anti-arrhythmic drugs (beta blockers)	19
Sex (male/female)	18/2
Atrial fibrillation	20
Hypertension	8
Diabetes mellitus	3
COPD	1

CVD: Cardiovascular Disease; **CABG:** Coronary Artery Bypass Grafting; **COPD:** Chronic Obstructive Pulmonary Disease; **PCI:** Percutaneous Coronary Intervention

Table 2: cMRI results before PVI

cMRI parameter	
LVEDD (mm)	51±5
LVESD (mm)	33±6
EDV (mL)	135±36
ESV (mL)	58±27
EF (%)	57±10
LV mass (g)	155±37
RVEDD (mm)	42±8

LVEDD: enddiastolic left ventricular diameter, **LVESD:** endsystolic left ventricular diameter, **EDV:** enddiastolic volume, ESV: endsystolic volume, **EF:** ejection fraction, **LV mass**: left ventricular mass, **RVEDD:** right ventricular enddiastolic diameter

Late gadolinium enhancement

Figure 3a-c represents cine loops in a short-axis view in a patient with hypertensive heart disease and LGE images with midwall fibrosis.

LGE indicated that no new myocardial scarring was present one month after PVI.

Global and circumferential strain

SENC images were obtained one day before PVI, one day after and one month after in four-chamber, two-chamber and short-axis views.

Figure 1d exhibits a representative example of left ventricle SENC measurement in a four-chamber view one day before PVI.

Figure 1d points out a presentative example of left ventricle SENC measurement in a short-axis view 1 day before PVI.

In four patients (20%), PVI resolved the wall motion abnormalities complete, in the other patients some little wall motion abnormalities persisted.

Global strain decreased significantly in four-chamber ($p<0.02$; Figure 4a) and two-chamber views ($p<0.02$) (Figure 4b) one month after PVI compared with one day before PVI.

The circumferential strain also decreased significantly in the four-chamber view ($p<0.03$; Figure 4c) one month after PVI compared with one day before PVI.

Follow-up

All 20 investigated patients pictured an increased quality of life from EHRA III to EHRA I. LGE indicated that no new myocardial scarring was present one month after PVI. All patients except one with tetralogy of Fallot were still on beta-blocker therapy one month after PVI. No adverse effects (e.g., atrial-oesophageal fistula) were detected [11].

DISCUSSION

In this study, we aimed to examine the functional recovery of the left ventricle from atrial fibrillation after PVI with the nMARQ system regarding the comparison of global and circumferential left ventricular wall motion with SENC. The patients were investigated one day prior, one day and one month after PVI with nMARQ.

Further, we assessed scar occurrence with LGE after the procedure and quality of life with EHRA before and one month after PVI.

We found that the nMARQ system was a safe method for performing the PVI procedure before the onset of heart failure symptoms in patients with symptomatic atrial fibrillation only on beta-blocker therapy, given that no adverse effects were detected (e.g., transoesophageal fistula) and quality of life was explicitly

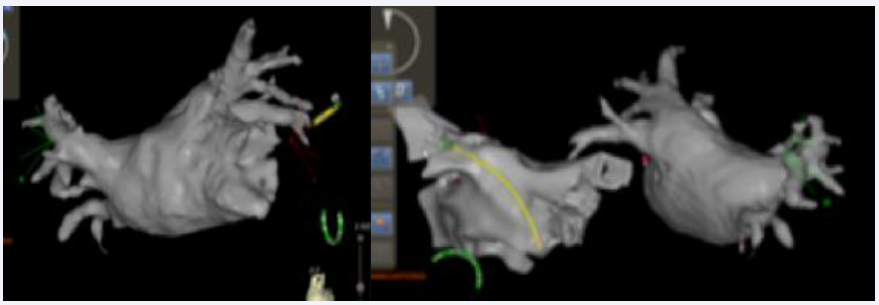

Figure 1a nMARQ system: representative image of the left atrium segmentation with pulmonary vein ostia using the nMARQ system in two different views.

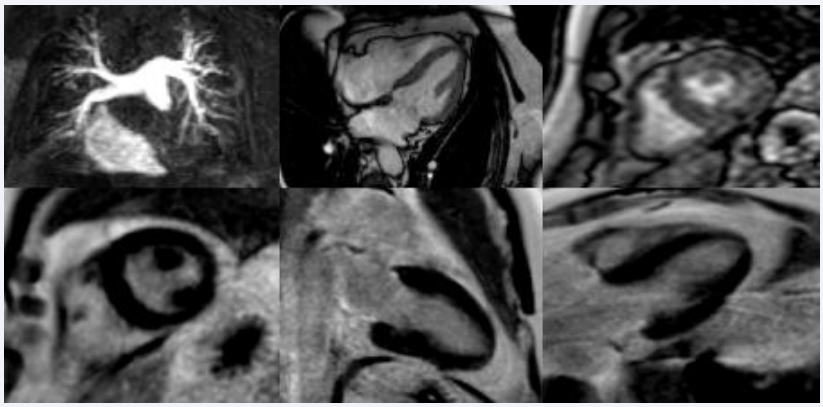

Figure 1b **Representative images obtained one day before PVI:** pulmonary veins as imaged by cMRI with angiography (upper left), four-chamber view in cine loops (upper middle) and SENC imaging in short-axis view (upper right). LGE images of pulmonary veins without fibrosis are shown in short-axis (lower left), two-chamber (lower middle) and four-chamber views (lower right).

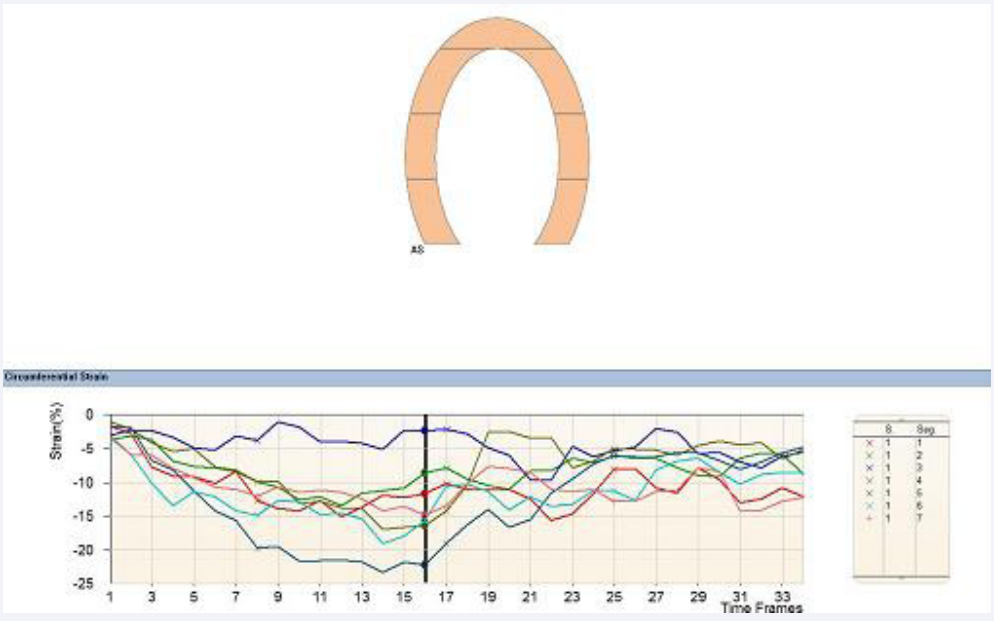

Figure 1c Representative example of left ventricle SENC measurement in a four-chamber view 1 day before PVI.

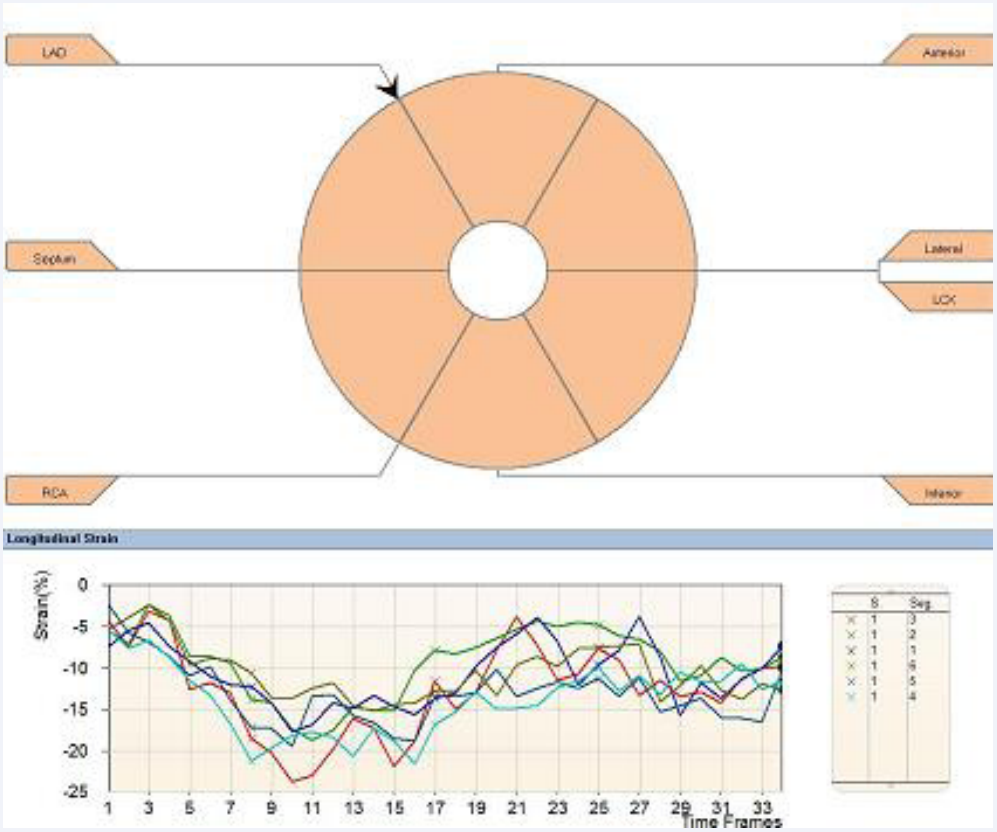

Figure 1d Representative example of left ventricle SENC measurement in a short-axis view 1 day before PVI. LAD: left anterior descending artery; LCX: left circumflex artery; RCA: right coronary artery.

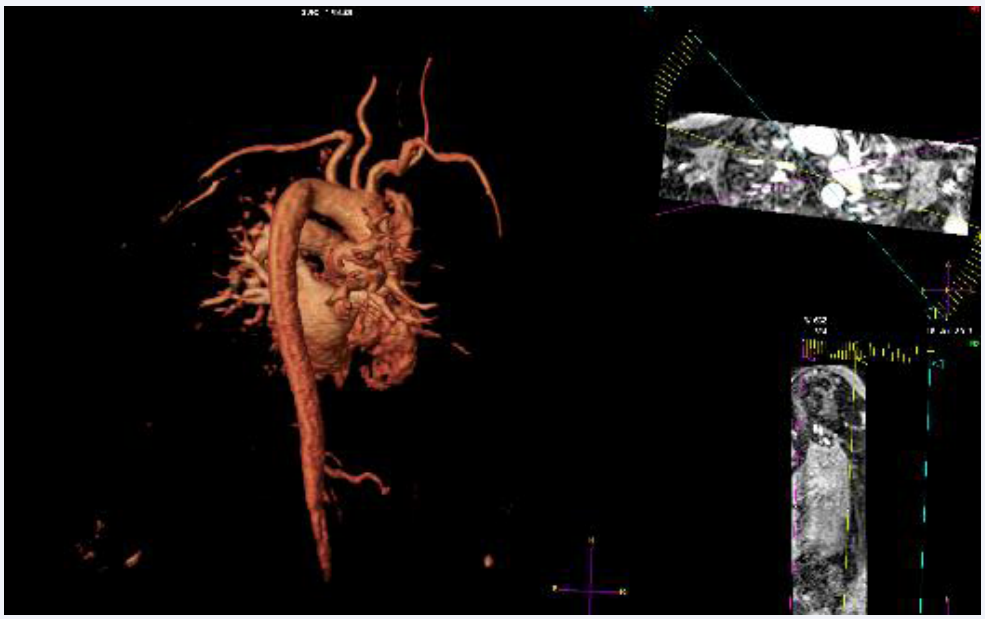

Figure 2a Representative digital subtraction angiography with reconstruction one day after PVI for identification of vein lesions.

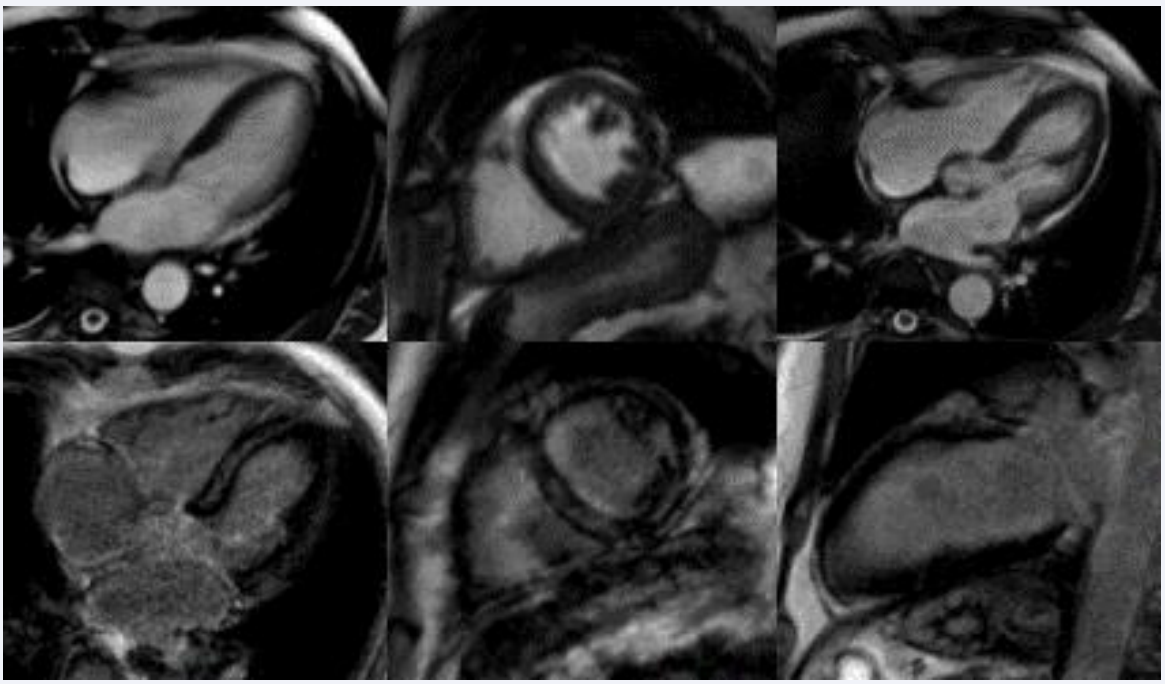

Figure 2b cMRI after PVI: four-chamber view on cine loop imaging (first), left ventricle (short-axis view) on cine loop imaging (second), "five-chamber" view featuring prominent trabeculations in a patient with hypertensive heart disease (third), and a four-chamber LGE image from a patient with midwall fibrosis in the left ventricle one day after PVI (fourth). On LGE, the left ventricle of the same patient (short-axis view) demonstrates discrete midwall fibrosis 1 day after PVI (fifth) and a lack of fibrotic areas in a two-chamber view 1 day after PVI (sixth).

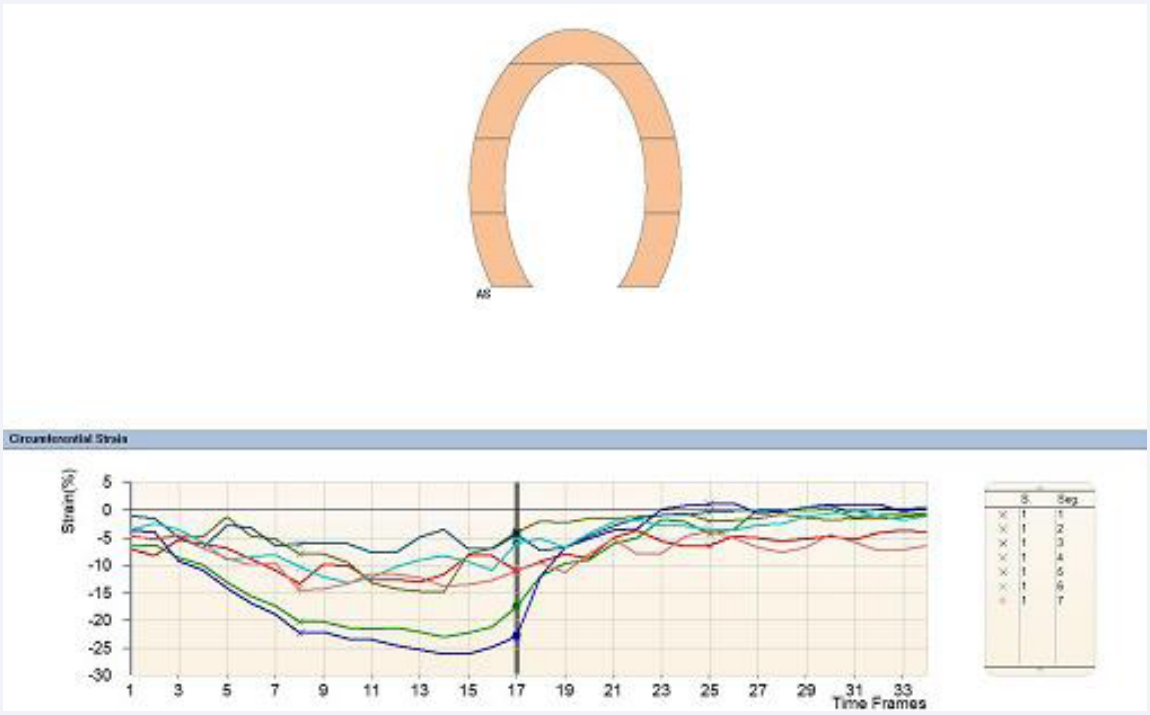

Figure 2c Representative example of left ventricle SENC measurement in a four-chamber view 1 day after PVI.

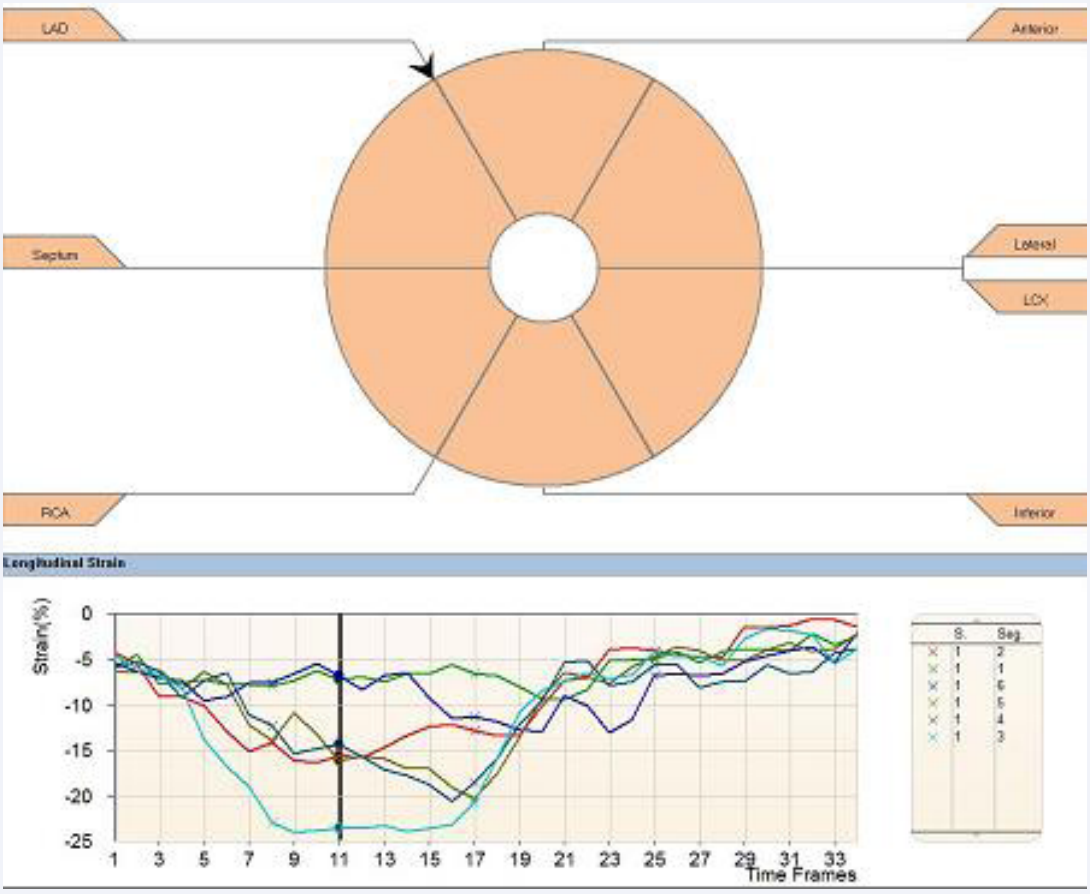

Figure 2d Representative example of left ventricle SENC measurement in a short-axis view 1 day after PVI. LAD: left anterior descending artery; LCX: left circumflex artery; RCA: right coronary artery.

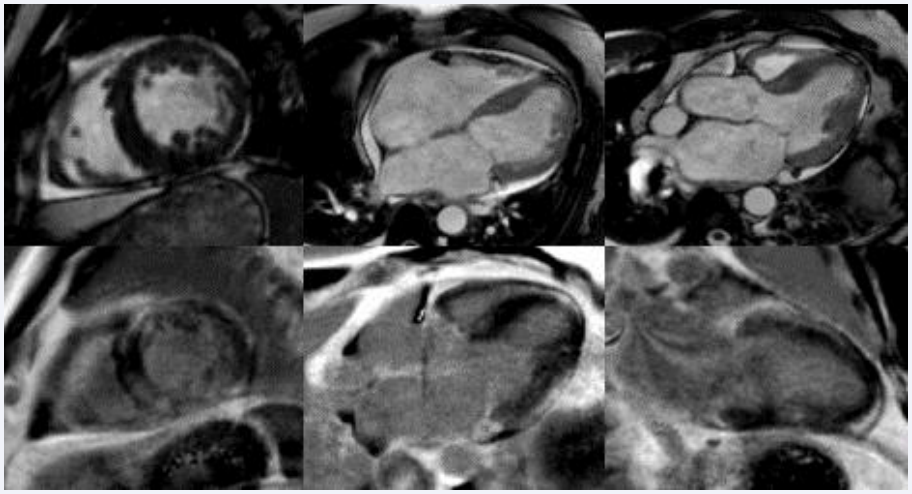

Figure 3a Cine loops in a short-axis view in a patient with hypertensive heart disease and increased myocardial mass (first); cine loop images in four-chamber (second) and three-chamber views (third). LGE in a patient with midwall fibrosis one month after PVI in short-axis view (left), three-chamber view (middle), and two-chamber view (right).

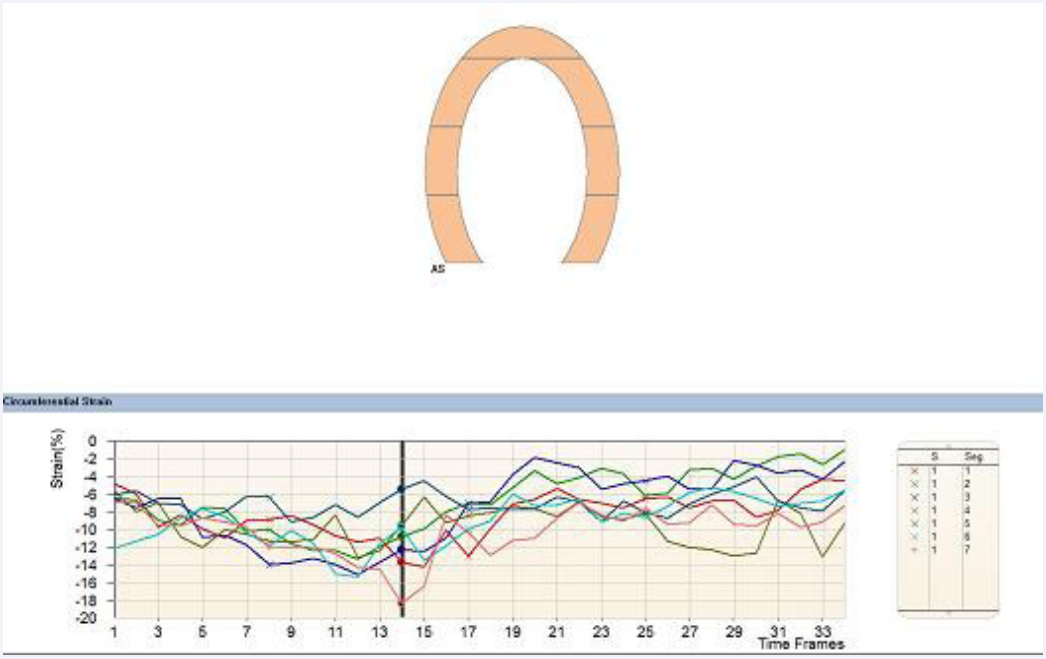

Figure 3b Representative example of left ventricle SENC measurement in a four-chamber view 1 month after PVI.

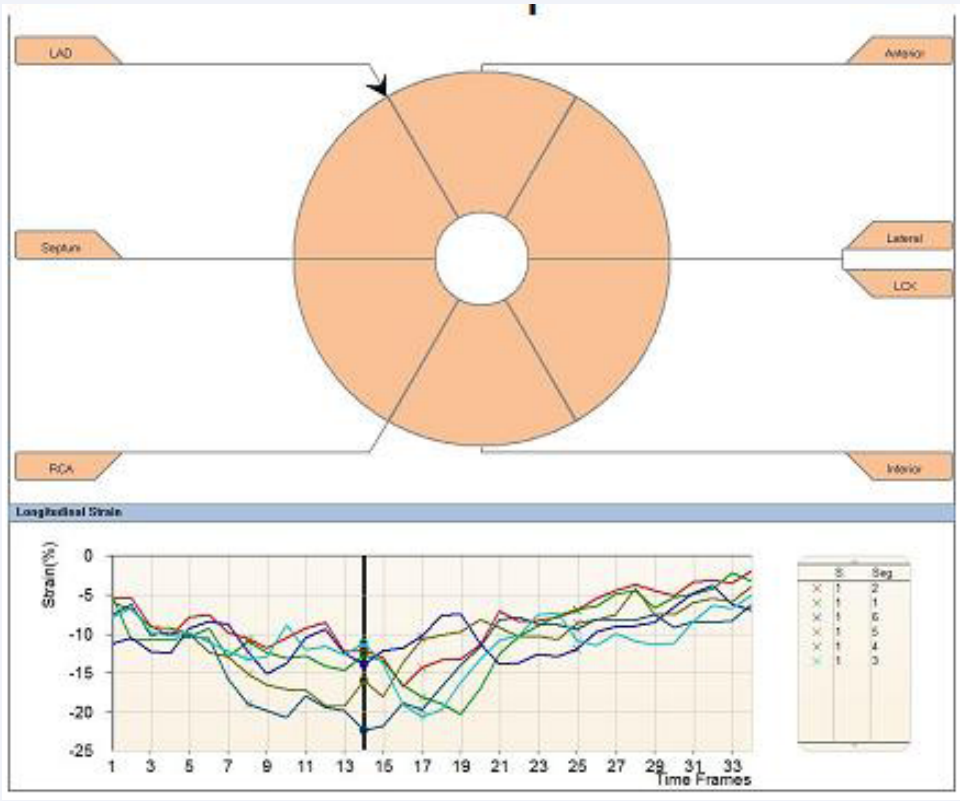

Figure 3c Representative example of left ventricle SENC measurement in short-axis view 1 day after PVI. LAD: left anterior descending artery; LCX: left circumflex artery; RCA: right coronary artery.

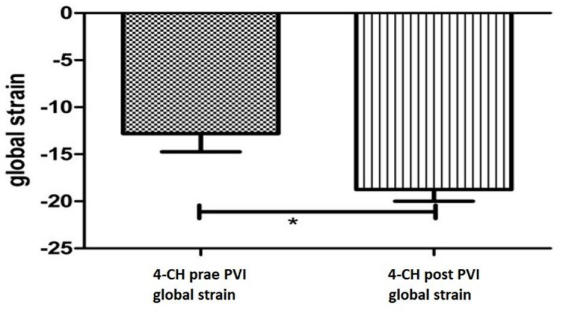

Figure 3a Global strain analysis of the left ventricle in a four-chamber view one day before and one month after PVI.

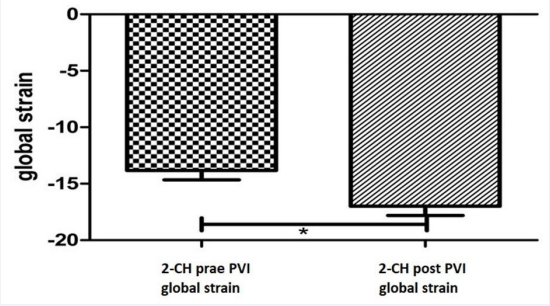

Figure 4b Global strain analysis of the left ventricle in a two-chamber view one day before and one month after PVI.

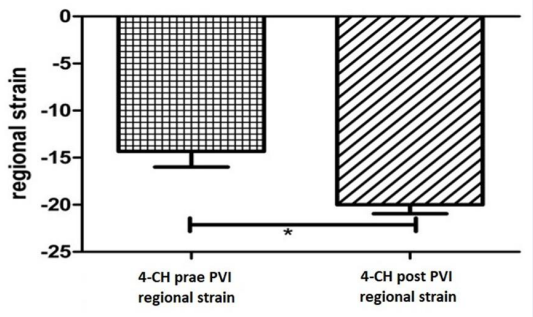

Figure 4c Circumferential strain analysis of the left ventricle in a four-chamber view 1 day before and 1 month after PVI.

increased. Our findings were in line with Mahida [12], who conducted a multi center study with the application of nMARQ in atrial fibrillation with one year follow up. Here, patients with drug refractory atrial fibrillation were included. They concluded that nMARQ is associated with short procedure times and high acute success rates.

Our data show that the nMARQ procedure results in improvements in global and circumferential strain. Specifically, there was a statistically significant difference in the improvement of regional wall motion abnormalities one month after PVI. Prior to this study, little was known about regional wall motion abnormalities before and after PVI in the left ventricle outside of the heterogeneous effects reported in healthy volunteers [9].

Moyer et al. [13], investigated the left atrium with tagging in cMRI in patients with atrial fibrillation and in healthy volunteers for setting up a functional system for the documentation of regional wall motion abnormalities.

The constitution of the left ventricle after PVI has not been extensively investigated yet.

Fortunately, we did not detect new scar formation after

PVI in the left ventricle one month after PVI. Another research group similarly observed that catheter ablation targeting the pulmonary veins in atrial fibrillation rarely achieves permanent encircling scars in the intended areas [14]. In another study that conducted cMRI follow-up on scar development in the left atrium following PVI found that increased left atrial thickening and oedema correlated with LGE scarring at 30 days [15]. Likewise, diffuse ventricular fibrosis has been documented with the aid of T1 mapping after PVI, which may explain the development of recurrent atrial fibrillation following the procedure [16].

A previous study used cMRI to compare three-year clinical outcomes after robotic versus standard catheter ablation. In that study, robotically assisted system ablation resulted in increased LGE around the pulmonary vein atrium, but effective lesions created through improved catheter stability and contact force during the initial procedure appeared to have a possible role in reducing subsequent re-operation [17]. Additionally, lesion formation was compared between an advanced cryoballoon and a standard cryoballoon. Ablation formation did not differ between the two techniques, but there was a significantly reduced rate of atrial fibrillation recurrence after three months with the Arctic Front cryoballoon [4].

LIMITATIONS

This study was limited by the small number of patients and the exclusion of patients due to cMRI contraindications, such as implanted permanent pacemakers and implanted cardioverter-defibrillators. Further studies should also include patients with cMRI compatible permanent pacemakers and implanted cardioverter-defibrillators.

CONCLUSION

Pulmonary vein isolation with nMARQ is a beneficial treatment for atrial fibrillation and brings about functional ventricular recovery by reinstating the sinus rhythm. Increased quality of life is attended by less wall motion abnormalities. Further work needs to be done to investigate the procedure over a longer period and increased patient numbers.

REFERANCES

1. Marcusohn E, Kobo O, Postnikov M, Epstein D, Agmon Y, Gepstein L. Left Ventricular Systolic Dysfunction Due to Atrial Fibrillation: Clinical and Echocardiographic Predictors. Card Fail Rev review. 2021; 7: e16.

2. Siebermair J, Silver M, Wakili R. Pulmonary Vein Isolation with the Multipolar nMARQTM Ablation Catheter: Efficacy And Safety In Acute And Long-Term Follow Up. J Atr Fibrillation. 2017; 9: 1600.

3. Calkins H, Hindricks G, Cappato R, Kim Y-H, Saad E B, Aguinaga L, et al. 2017 HRS/EHRA/ECAS/APHRS/SOLAECE expert consensus statement on catheter and surgical ablation of atrial fibrillation. Europace. 2018; 20: e1-e160.

4. Halbfass PM, Mitlacher M, Turschner O, Brachmann J, Mahnkopf C. Lesion formation after pulmonary vein isolation using the advance cryoballoon and the standard cryoballoon: Lessons learned from late gadolinium enhancement magnetic resonance imaging. Europace. 2015; 17: 566-573.

5. Arujuna A, Karim R, Zarinabad N, Gill J, Rhode K, Schaeffter T, et al. A randomized prospective mechanistic cardiac magnetic resonance study correlating catheter stability, late gadolinium enhancement and 3 year clinical outcomes in robotically assisted vs. Standard catheter ablation. Europace. 2015; 17: 1241-1250.

6. Ananthapadmanabhan S, Nguyen T, G Vo, Dimitri H, Otten J. Direct comparison of multilayer left ventricular global strain using CMR feature tracking and speckle tracking echocardiography. BMC Cardiovasc Disord. 2021; 21: 107.

7. Seo Y, Ishiyu T, Anouma K. Current status of 3-Dimensional Speckle Tracking Echocardiography: A Review from our Experiences. J Cardiovasc Ultrasound. 2014; 22: 49-57.

8. Ananthapadmanabhan S, Nguyen T, Vo G, Dimitri H, Otten J. Direct comparison of multilayer left ventricular global strain using CMR feature tracking and speckle tracking echocardiography. BMC Cardiovasc Disord. 2021; 21: 107.

9. Osman NF. Detecting stiff masses using strain-encoded (SENC) imaging.Magn Reson Med. 2003; 49: 605-608.

10. Neizel M, Korosoglou G, Lossnitzer D, Kuehl H, Hoffmann R, Ocklenburg C. Impact of systolic and diastolic deformation indexes assessed by strain-encoded imaging to predict persistent severe myocardial dysfunction in patients after acute myocardial infarction at follow-up. J Am Coll Cardiol. 2010; 56: 1056-1062.

11. Calkins H, Hindricks G, Cappato R, Kim Y-H, Saad E B, Aguinaga, et al. 2017 HRS/EHRA/ECAS/APHRS/SOLAECE expert consensus statement on catheter and surgical ablation of atrial fibrillation. Europace. 2018; 20: e1-e160.

12. Mahida S, Hooks D, Nentwich K, Andre G, Grimaldi M, Shin DI, et al. nMARC Ablation for Atrial Fibrillation: Results from a Multicenter Study. J Cardiovasc Electrophysiol. 2015; 26: 724-729.

13. Moyer C, Helm P, Clarke C, Budge L, Kramer C, Ferguson J, et al. Wall-Motion Based Analysis of Global and Regional Left Atrial Mechanics. IEEE Trans Med Imaging. 2013; 32: 1765-1776.

14. Akoum N, Wilber D, Hindricks G, Jais P, Cates J, Marchlinski F, et al. MRI assessment of ablation-induced scarring in atrial fibrillation: Analysis from the DECAAF study. J Cardiovasc Electrophysiol. 2015; 26: 473-480.

15. Hsing J, Peters DC, Knowles BR, Manning WJ, Josephson ME. Cardiovascular magnetic resonance imaging of scar development following pulmonary vein isolation: A prospective study. PLoS One. 2014; 9: e104844.

16. McLellan AJ, Ling LH, Azzopardi S, Ellims AH, Iles LM, Sellenger MA, et al. Diffuse ventricular fibrosis measured by T1 mapping on cardiac MRI predicts success of catheter ablation for atrial fibrillation. Circ Arrhythm Electrophysiol. 2014; 7: 834-840.

17. Arujuna A, Karim R, Zarinabad N, Gill J, Rhode K, Schaeffter T, et al. A randomized prospective mechanistic cardiac magnetic resonance study correlating catheter stability, late gadolinium enhancement and 3 year clinical outcomes in robotically assisted vs. Standard catheter ablation. Europace. 2015; 17: 1241-50.